Interaction of Water Molecules with Cytosine Tautomers: An Excited-State Quantum Chemical Investigation

M. K. Shukla and Jerzy Leszczynski*

Computational Center for Molecular Structure and Interactions, Department of Chemistry, Jackson State University, 1400 J. R. Lynch Street, Jackson, Mississippi 39217

Received: May 31, 2002; In Final Form: September 3, 2002

A detailed theoretical study of molecular geometry and electronic spectra was performed for four cytosine tautomers (amino−oxo (N1H and N3H), amino−hydroxy, and imino−oxo) and their hydrated forms with three water molecules. Geometries were optimized both in the ground and lowest singlet $\pi\pi^*$ and $n\pi^*$ excited states without any symmetry restriction. Ground-state geometries were optimized at the Hartree−Fock level of theory, whereas excited states were generated employing the configuration interaction technique involving singly excited configurations (CIS method). This was followed by excited-state geometry optimization. The nature of the corresponding potential energy surfaces was ascertained with the help of harmonic vibrational frequency analysis. All geometries were found to be minima at the respective potential energy surfaces. For the N1H tautomer, the ground-state geometry was also optimized at the B3LYP level, and the optimized geometry was used for the excitation energy calculation from the time-dependent density functional theory (TDDFT) method. The 6-311G(d,p), 6-311++G(d,p), and aug-cc-pVTZ basis sets were used in the study. However, in some singlet $\pi\pi^*$ excited-state geometry optimizations, the 4-31G basis set was used for all atoms except the amino nitrogen, for which the 6-311+G(d) basis set was used. Although, ground-state geometries of all tautomers were found to be planar except for the amino group, corresponding excited-state geometries were found to be appreciably nonplanar. The mode of interaction of water molecules with cytosine tautomers was found to be different in the singlet $n\pi^*$ excited state as compared to the ground and singlet $\pi\pi^*$ excited states. Furthermore, in the gas phase and under hydration, cytosine is suggested to phototautomerize to the N3H tautomeric form.

1. Introduction

A detailed understanding of the physicochemical properties of nucleic acid polymers demands explicit knowledge of the structures and interactions of constituent nucleic acid bases. The possible role of rare tautomers of these bases in spontaneous mutation has motivated various theoretical and experimental investigations to understand the mechanism of formation of minor tautomers in different environments.[1−15] Cytosine is one of the fundamental building blocks of nucleic acid polymers and has been studied extensively both theoretically and experimentally.[1−7,10,11,16−21] Among natural nucleic acid bases, it is also next to guanine, which possesses several tautomeric structures under different environmental conditions.[1−7,16−21] Thus, at low temperature in the argon and nitrogen matrixes, it exists as a mixture of amino−hydroxy and N1H amino−oxo tautomeric forms in comparable amounts, the equilibrium being shifted slightly to the former tautomeric form.[16,17] The existence of the imino−oxo tautomeric form has been also indicated in the matrix isolation study of 1-methylcytosine.[18] Here it should be noted that the microwave study has yielded rotational constants for three tautomers, namely, amino−oxo, imino−oxo, and amino−hydroxy tautomers of cytosine.[19] Furthermore, whereas in aqueous solution both of the amino−oxo forms (N1H and N3H) are present,[20] under crystalline environments it exists mainly in the N1H amino−oxo form.[21] High-level quantum chemical theoretical calculations yielded small energy differences between different tautomers, and such energy differences are found to be extremely sensitive to levels of approach, giving rise to somewhat contradictory results.[22−25] For example, to predict the correct relative stability of different tautomers at the coupled-cluster level, an approach with single, double, and triple excitations (CCSD(T)) is necessary.[22] Generally, MP2 and CCSD(T) levels reveal similar trends,[22,23] but nothing concrete can be arrived at even at the different levels of the PMn treatment.[23] Although, the DFT method provides excellent agreement with the experimental rotational constants and vibrational frequencies, it differs with regard to the computed relative stability of different tautomers obtained at the CCSD-(T) and PMn levels of theory.[22−25]

From different experimental measurements, one may conclude that DNA is heavily hydrated.[26−30] Such hydration plays an important role in the stabilization of 3D structures of nucleic acid polymers. Different theoretical investigations have been performed to study the interactions of water molecules with cytosine tautomers.[23,31−34] It has been found that under such hydrations the N1H amino−oxo tautomer is the most stable in the ground state. This result agrees with experiment.[20] The barrier height of tautomerization is also found to decrease substantially when a water molecule is present in the proton-transfer reaction path.[31] Recently, Shishkin et al.[32] have studied the interaction of cytosine with 14 water molecules at the B3LYP/6-31G(d) level. They have found that under such massive hydration the structure of cytosine can be described as

* Corresponding author. E-mail: jerzy@ccmsi.us.

10.1021/jp021317j CCC: $22.00
Published on Web 10/19/2002

a superposition of the amino−oxo and zwitterionic imino−hydroxy resonance structures.

Among pyrimidines, cytosine is photophysically the second most active after thymine in view of the photodimerization reaction.[10,11] To the best of our knowledge, experimental data concerning excited-state geometries of cytosine is not available. In fact, there is no direct experimental method to determine the excited-state geometry of such a complex molecular system. However, the supersonic-jet-cooled spectroscopic and resonance Raman studies of uracil and thymine have indicated the nonplanar excited-state geometries.[35,36] Such predictions are also validated by theoretical calculations.[37] Geometry optimization calculations using the AM1 Hamiltonian on the lowest excited dimer (excimer) singlet state of cytosine predicted 3 kcal/mol of binding energy.[38] The excimer geometry was found to be distorted, with the C5C6 bonds of two planes in close contact. However, for the planar structure and in the triplet state, the excimer was predicted to be unstable.[38] Although there are plenty of data for cytosine−water interactions in the ground state, such a study for excited states has not been yet performed. Such an interaction study is very important since water molecules play an important role in structural stabilization and electronic excitation has a significant effect on hydrogen-bonding structures. For example, hydrogen bonds are found to be largely destabilized in the nπ* excited state.[39−41] In an experimental study on the indole−water interaction, the orientation of the water molecule was found to change with the excitation, and the hydrogen bond strength was also found to increase.[42] A recent experimental study on hydrated clusters of adenine in a supersonic molecular beam shows the weakening of hydrogen bonding and subsequent fragmentation of adenine monomer hydrated clusters in the nπ* excited state.[41] In an earlier study of cytosine, only the N1H amino−oxo tautomer was considered, and the interaction with water molecules was not investigated.[37] Recently, solute−solvent hydrogen bonds in nucleic acid bases have been suggested to be responsible for the rapid vibrational cooling of the vibrationally excited ground state.[12] In the present study, we have performed an excited-state geometry optimization study of cytosine tautomers and their interaction with water molecules. The possible mechanism for the phototautomerization is also investigated.

2. Computational Details

Ground-state geometries were optimized using the ab initio-restricted Hartree−Fock level of theory. Excited states were generated using the configuration interaction considering single-electron excitations (CIS) from the filled to the unfilled molecular orbitals using the optimized ground-state geometry, and this was followed by geometry optimization in different singlet excited states.[43] The standard 6-311G(d,p) basis set was used; however, in some of the excited-state geometry optimizations, a combination of 4-31G and 6-311+G(d) basis sets was used. The nature of the corresponding ground- and excited-state optimized potential energy surfaces (PES) was analyzed by the harmonic vibrational frequency calculations, and all optimized structures were found to be minima on the respective PES. For the N1H tautomer, the ground-state geometry was also optimized at the B3LYP level using the 6-311G(d,p) and 6-311++G(d,p) basis sets. The B3LYP-optimized geometry was used for the vertical transition energy calculations in the time-dependent density functional theory (TDDFT)[44] emplying the 6-311G(d,p), 6-311++G(d,p), and aug-cc-pVTZ basis sets. The B3LYP functional was used in the TDDFT calculation. All calculations were performed using the Gaussian 94 and Gaussian 98 suites of programs.[45]

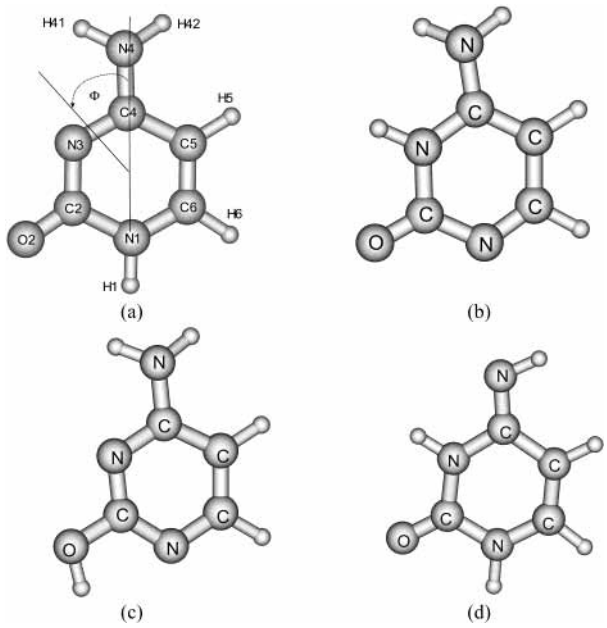

Figure 1. Four tautomers of cytosine: (a) N1H, (b) N3H, (c) enol, (d) imino. The Φ shows the transition-moment direction according to the Tinoco−DeVoe convention.

3. Results and Discussion

3.1. Ground State. The four tautomers of cytosine, namely, N1H, N3H, enol, and imino, and their hydrated forms with three water molecules were considered for the study (Figures 1 and 2). The selection of the tautomers was based on their existence in different environments. For example, N1H and N3H tautomers are present in an aqueous environment,[20] the enol form dominates in low-temperature matrixes,[16,17] and the presence of the imino form is indicated in the low-temperature study of 1-methylcytosine.[18] The zero-point-energy (ZPE)-corrected relative total energies of these tautomers shown in Table 1 suggest the following stability order: enol > N1H > imino > N3H.

This prediction is in accordance with earlier results obtained with the electron-correlated methods such as MP2 and CCSD-(T), which are also shown in Table 1.[7,22,23] We have used the supermolecular approach to study the effect of the aqueous environment. Experimental study of uracil has suggested the binding of three water molecules in the first solvation shell.[46] We have considered three water molecules for the hydration of cytosine tautomers in the first solvation shell (Figure 2). The relative energies of hydrated tautomers (Table 1) suggest following stability order: N1H > enol > imino > N3H.

Thus, whereas the enol tautomer is the most stable in the gas phase, the N1H tautomer is the most stable under hydration. The change in the stability order is in accordance with the experimental findings that in aqueous environments the N1H form is the most stable whereas in low-temperature matrixes the enol form dominates.[16−20] Furthermore, the imino and enol tautomers are largely destabilized whereas the N3H tautomer is stabilized after hydration (Table 1). The predicted order of the tautomeric stability after hydration is also in agreement with the theoretical results on the stability of cytosine tautomers in an aqueous medium at the MP2/6-31++G(d,p) level (Table 1) obtained by Sambrano et al.[7] using the continuum model in which multipolar expansions in an ellipsoidal cavity are employed. These results suggest that the hydration of cytosine

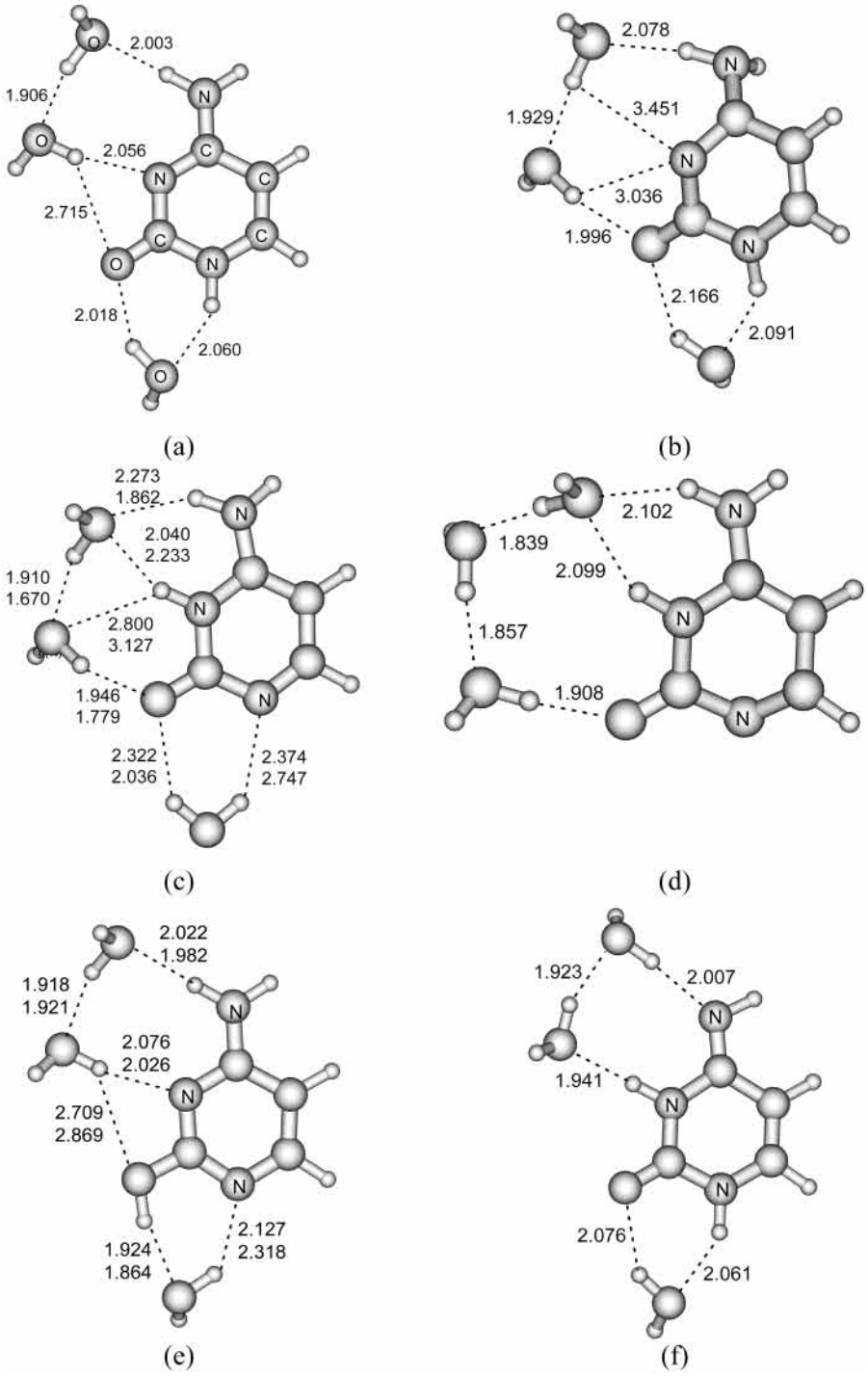

Figure 2. Structure and hydrogen bond lengths of three water complexes of cytosine tautomers: (a) N1H tautomer in the ground state, (b) N1H tautomer in the $S_2(n\pi^*)$ excited state, (c) N3H tautomer in the ground state (top index) and $S_1(\pi\pi^*)$ excited state (bottom index), (d) N3H tautomer in the $S_2(n\pi^*)$ excited state, (e) enol tautomer in the ground state (top index) and $S_1(\pi\pi^*)$ excited state (bottom index), and (f) imino tautomer in the ground state.

tautomers with three water molecules is a good approximation to account for the qualitative effect of the aqueous environment. It should be mentioned here that our aim is not to discuss the ground state in detail, but we will rather discuss detailed properties of excited states. The ground-state properties of different tautomers have already been studied by different investigators using more sophisticated theoretical methods, as discussed earlier.[1−7]

3.2. Vertical Transitions. The TDDFT method has been suggested to be a reliable tool with which to study electronic transitions of molecules.[44] It offers a relatively cost-effective and efficient method to produce electronic transitions comparable to experimental data, and unlike the CIS method, a linear scaling of transition energies is not needed. Furthermore, it offers some dynamic electron correlation for excited-state calculations.[44] The computed vertical singlet $\pi\pi^*$ and $n\pi^*$ transition energies of the N1H tautomer at different basis sets (6-311G(d,p), 6-311++G(d,p), and aug-cc-pVTZ) for the B3LYP/6-311G(d,p) and B3LYP/6-311++G(d,p) reference geometries are presented in Table 2. It has been found that higher-energy transitions are highly contaminated with Rydberg-type orbitals. The quantitative assignments for such transitions lying at higher

TABLE 1: Relative Total Energy (ΔE, kJ/mol) of Different Tautomers of Cytosine and Their Complexes with Three Water Molecules with Respect to the N1H Form and Dipole Moment (μ, D) at the HF/6-311G(d,p) Level

		ΔE						
				earlier results[a]				
tautomer	μ[a]	isolated form	hydrated form	CCSD (T)[b]	MP4[c]	MP2[d]	MP2[e]	water[f]
N1H	6.98	0.0	0.0	0.0	0.0	0.0	0.0	0.0
N3H	8.15	29.41	23.60		31.38	29.29	30.80	26.28
enol	3.34	−5.38	11.29	−6.08	0.84	−9.20	−6.40	23.10
imino	5.12	3.89	19.16	1.38	3.35	8.79	7.45	24.43

[a] Corresponds to isolated cytosine tautomers. [b] At the CCSD(T)/cc-pvtz(-f)//MP2/cc-pvtz(-f) level; see ref 22. [c] At the MP4(SDQ)/6-31+G(d,p)//MP2/6-31G(d) level; see ref 23. [d] At the MP2/6-311++G(d,p)//MP2/6-31G(d) level; see ref 23. [e] At the MP2/6-31++G(d,p) level; see ref 7. [f] At the MP2/6-31++G(d,p) level continuum model that uses multipolar expansions in an ellipsoidal cavity; see ref 7.

TABLE 2: Vertical $\pi\pi^*$ and $n\pi^*$ Excitation Energies (ΔE, eV) and Oscillator Strengths (f) of the N1H Tautomer of Cytosine and Its Hydrated Form Obtained by the TDDFT Method

TDDFT/6-311G(d,p)[a]				TDDFT/6-311G(d,p)[b]		TDDFT/6-311++G(d,p)[b]				TDDFT/aug-cc-pVTZ[b]	
isolated		hydrated		isolated		isolated		hydrated		isolated	
ΔE	f	ΔE	f	ΔE	f	ΔE	f	ΔE	f	ΔE	f
$\pi\pi^*$ Transitions											
4.72	0.037	4.90	0.054	4.70	0.036	4.64	0.043	4.82	0.059	4.62	0.043
5.55	0.088	5.47	0.090	5.53	0.089	5.43	0.086	5.39	0.099	5.42	0.082
$n\pi^*$ Transitions											
4.79	0.001	5.23	0.003	4.78	0.001	4.77	0.001	5.22	0.005	4.75	0.001
5.16	0.001	5.56	0.005	5.13	0.001	5.11	0.001	5.54	0.001	5.12	0.000

[a] At the B3LYP/6-311G(d,p) reference geometry. [b] At the B3LYP/6-311++G(d,p) reference geometry.

energy are therefore not feasible because of the unreliability of such assignments even at the TDDFT/aug-cc-pVTZ basis-set level. Therefore, only the two lowest singlet $\pi\pi^*$ and $n\pi^*$ transitions are presented in Table 2. The corresponding transitions for the hydrated species are also shown in the same Table. This Table shows that for the isolated species (unhydrated), the reference geometry has a negligible influence on the transition energy, which is evident from the results obtained at the TDDFT/6-311G(d,p)//B3LYP/6-311G(d,p) and TDDFT/6-311G(d,p)//B3LYP/6-311G++(d,p) levels of calulation. Although $\pi\pi^*$ transition energies are decreased by about 0.1 eV in going from the TDDFT/6-311G(d,p) to the TDDFT/6-311++G(d,p) level, such an effect for the $n\pi^*$ transition energies is not revealed (Table 2). Furthermore, Table 2 suggests that the transition energies converg even at the TDDFT/6-311++G(d,p) level. After hydration with three water molecules, the first $\pi\pi^*$ transition is blue-shifted whereas the second one is red-shifted compared to the corresponding transitions of the isolated species. Significantly large blue shifts are revealed in the $n\pi^*$ transitions after the hydration of the cytosine N1H tautomer (Table 2).

The computed vertical singlet low-energy $\pi\pi^*$ and two $n\pi^*$ transition energies of cytosine tautomers in the gas phase and after hydration obtained at the CIS/6-311G(d,p)//HF/6-311G(d,p) level are presented in Table 3. It should be noted that some transitions of the $\pi\sigma^*$/Rydberg type were also obtained. Because of the uncertain assignment and possibly significant basis-set dependence, we do not give them in the Table. To compare with experimental data and earlier theoretical results, the scaled (scaling factor 0.72)[40] transition energies along with some relevant experimental data[47−50] and CASPT2/CASSCF[51] transition energies are also presented in Table 3. For all tautomers, the lowest singlet transition is predicted to be the $\pi\pi^*$ type, and the second singlet transition is the $n\pi^*$ type. The first $n\pi^*$ transition of the N1H and N3H tautomers is mainly localized at the N1 and N3 atoms, respectively. The second singlet $n\pi^*$ transitions of the N1H and N3H tautomers are mainly localized at the carbonyl oxygen. However, Petke et al.[52] have suggested the participation of lone pairs of both of the N3 atom and carbonyl oxygen in the lowest two singlet $n\pi^*$ transitions of the N1H tautomer of the cytosine. Both of the $n\pi^*$ transitions of the enol form are localized at the N1 and N3 sites, whereas for the imino form they are localized at the carbonyl oxygen and imino nitrogen. Similar results have also been revealed for the N1H tautomer at the TDDFT level (Table 2).

Data shown in Table 3 suggest that the observed spectral transitions of cytosine in water can be explained in terms of the scaled transitions of the hydrated N1H tautomer within an accuracy of 0.2 eV, except for the second transition for which the error is about 0.3 eV. However, such an error is smaller if the comparison is made between the computed transitions of the hydrated N1H tautomer near 4.65, 5.58, 6.06, and 6.65 eV and the observed transitions of cytosine sublimed film near 4.54, 5.40, 6.07, and 6.67 eV.[50] It appears that the absorption peak of cytosine near 212 nm (5.85 eV) in water[47,48] is shifted to 6.07 eV in the sublimed-film experiment.[50] Such a difference between the computed and experimental data is not unexpected since the general features of the cytosine spectrum are found to be solvent-dependent.[10,47−50,53] The computed $\pi\pi^*$ transitions by the TDDFT method are also in close agreement with the experimental data and the CASPT2 results (Tables 2 and 3). The computed $n\pi^*$ transitions of the N1H tautomer lie near 5.02 and 5.4 eV, and the corresponding transitions for the hydrated species are near 5.37 and 5.71 eV (Table 3). The existence of $n\pi^*$ transition near 5.33 and 5.58 eV in cytosine has been indicated in different experimental and theoretical investigations.[37,48,49,51,54,55] The TDDFT computations of the hydrated species also show $n\pi^*$ transitions near 5.2 and 5.5 eV (Table 2). Therefore, our theoretical predictions are in close agreement with experimental results. Clark's group, with the help of polarized reflection spectroscopy of single crystals of cytosine monohydrate, assigned the transition-moment direction for the first three transitions explicitly and gave two possible values for the fourth transition.[48] The predicted angle of 6° with respect to the N1C4 direction (Figure 1a) for the first transition by Clark's group[48] is in accordance with 9° of Callis and Simpson[56] and 10° of Lewis and Eaton.[57] These authors[48] have

TABLE 3: Vertical $\pi\pi^*$ and $n\pi^*$ Excitation Energies (ΔE, eV), Oscillator Strengths (f), Transition Moment Directions (Φ, deg), and Dipole Moments (μ, D) of Cytosine Tautomers and Their Hydrated Forms at the CIS/6-311G(d,p)//HF/6-311G(d,p) Level[a]

						experimental data[b]							
isolated			hydrated		CASPT2/CASSCF[c]	Abs[1]		Abs[2]			Abs[3]	Abs[4]	
ΔE	f/Φ	μ	ΔE	f/Φ	$\Delta E^1/\Delta E^2/f/\Phi/\mu$	ΔE	f	ΔE	f	Φ	ΔE	ΔE	f
N1H Tautomer													
$\pi\pi^*$ Transitions													
6.32	0.171	5.60	6.46	0.221									
(4.55)	24		(4.65)	15	4.39/5.18/0.061/60.6/4.7	4.64	0.096	4.66	0.14	6	4.57	4.54	0.058
7.84	0.382	6.73	7.75	0.365									
(5.64)	−20		(5.58)	−19	5.36/6.31/0.108/−1.5/7.0	5.21	0.100	5.39	0.03	−46	5.34	5.40	0.073
8.42	0.686	7.06	8.41	0.649									
(6.06)	−48		(6.06)	−49	6.16/7.30/0.863/−39.7/6.2	5.83	0.211	5.85	0.13	76	5.77	6.07	0.115
9.49	0.167	6.74	9.23	0.293									
(6.83)	17		(6.65)	19	6.74/7.82/0.147/14.9/9.3	6.46	0.639	6.29	0.36	X	6.26	6.67	0.072
$n\pi^*$ Transitions													
6.97	0.003	4.28	7.46	0.007									
(5.02)			(5.37)		5.00/5.13/0.005/−/4.7								
7.50	0.001	3.73	7.93	0.000									
(5.40)			(5.71)		6.53/7.14/0.001/−/6.4								
N3H Tautomer													
$\pi\pi^*$ Transitions													
5.83	0.308	8.12	5.90	0.351									
(4.20)	−2		(4.25)	−6		4.29	0.198						
7.96[d]	0.152	5.57	7.89	0.303									
(5.73)	−87		(5.68)	−86		5.47	0.275						
8.04	0.215	6.55											
(5.79)	−85												
9.26	0.105	6.86	9.15	0.483									
(6.67)	−60		(6.59)	−62									
9.34	0.372	7.42											
(6.72)	−72												
9.60	0.293	8.14	9.62	0.334									
(6.91)	42		(6.93)	50									
$n\pi^*$ Transitions													
6.24	0.004	5.36	6.66	0.003									
(4.49)			(4.80)										
7.31	0.001	5.53	7.84	0.021									
(5.26)			(5.64)										
Imino Tautomer													
$\pi\pi^*$ Transitions													
6.62	0.560	4.74	6.57	0.250									
(4.77)	−7		(4.73)	−6		4.64	(0.17)						
8.29	0.143	2.97	8.18	0.196									
(5.97)	17		(5.89)	15		5.59	(0.39)						
9.06	0.214	5.21	8.94	0.181									
(6.52)	27		(6.44)	56									
9.51	0.558	4.64	9.36	0.587									
(6.85)	−47		(6.74)	−33									
$n\pi^*$ Transitions													
7.13	0.005	4.53	7.55	0.004									
(5.13)			(5.44)										
8.03	0.000	4.18	8.15	0.007									
(5.78)			(5.87)										
Enol Tautomer													
$\pi\pi^*$ Transitions													
6.53	0.202	3.55	6.47	0.250									
(4.70)	−9		(4.66)	−12									
7.41	0.088	3.38	7.47	0.130									
(5.34)	47		(5.38)	35									
8.74	0.522	2.88	8.73	0.492									
(6.29)	−77		(6.29)	−86									
9.03	0.844	3.75	8.98	0.893									
(6.50)	3		(6.47)	−6									
$n\pi^*$ Transitions													
7.00	0.008	1.12	7.32	0.007									
(5.04)			(5.27)										
7.92	0.001	3.14	8.20	0.002									
(5.70)			(5.90)										

[a] Scaled (scaling factor 0.72) excitation energies are in parentheses. [b] Abs[1]: absorption transitions of cytosine in water and experimental data for N3H and imino tautomers correspond to 3-methylcytosine and 3-methylcytidine, respectively, obtained in aqueous solution at pH 11 (ref 47); Abs[2]: absorption transitions of cytosine in water; the Φ values are based on the polarized spectra of the cytosine crystal, and X = −27 or 86 (ref 48); Abs[3]: absorption transitions of cytidine in water (ref 49); Abs[4]: absorption transitions of sublimed cytosine (ref 50). [c] ΔE^1: CASPT2 energy; ΔE^2: CASSCF energy; see ref 51. [d] Rydberg contamination.

suggested that the predicted discrepancy in the transition-moment direction obtained in linear dichroism studies of cytosine and related compounds[58,59] dissolved in stretched poly(vinyl alcohol) films can be removed if the orientational axis for the stretched film is rotated, and under such a rotation, LD results were found to be in accordance with the crystal results.[48] Clark's group[48] have suggested that the transition-moment direction with respect to the N1C4 direction (Figure 1a) for bands II, III, and IV would be −46, 76, and −27 or 86°, respectively. Such a conclusion regarding transition-moment directions for transitions II and III was based on polarized fluorescence work on 5-methylcytosine,[60] which predicted that the angle between the moments of I and II is 40 ± 15°. Similar results were also found for cytosine monophosphate.[61] The stretched-film work[58,59,62] indicated that the angle between I and III is larger than that between I and II. Furthermore, Clark's group[48] have questioned the selection of the orientational axis by Bott and Kurucsev[59] and have suggested that the orientational axis should be −9°, in contrast to the −38° selected by them.[59] Under such circumstances, the predicted values by Bott and Kurucsev[59] have been shown to be in accordance with predictions made by Clark and co-workers.[48] The CIS computed transition-moment directions for the first four $\pi\pi^*$ transitions of the N1H tautomer are found to be 24, −20, −48, and 17°, and the corresponding values for hydrated species are 15, −19, −49, and 19° (Table 3). Although our computed transition-moment directions differ from the values predicted by Clark group,[48] they are in accordance with the predicted angle of 40 ± 15° between transitions I and II.[60] Furthermore, our computed transition-moment directions show that the angle between transitions I and III is larger than the angle between transitions I and II, agreeing with stretched-film studies.[58,59,62]

The comparison of the lowest singlet $\pi\pi^*$ transition of cytosine tautomers presented in Table 3 suggests that with respect to the N1H tautomer, the transition for the N3H tautomer is appreciably red-shifted for both the isolated and hydrated forms. Whereas in the case of the enol and imino tautomers the isolated forms show a blue shift with respect to the isolated form of the N1H tautomer, for hydrated species, the imino form shows slight blue shift, and the enol form does not show any shift with respect to the N1H form (Table 3). The observed red shift in the first $\pi\pi^*$ transition of the N3H tautomer is in accordance with experimental observations that the aqueous absorption spectra of 3-methylcytosine show a significant red shift, with the peak near 289 nm (4.29 eV) as compared to the corresponding peak of cytosine observed near 266 nm (4.66 eV).[47] Furthermore, the observed transitions of 3-methylcytosine near 4.29 and 5.47 eV can be explained in terms of the computed transitions of hydrated forms of the N3H tautomer near 4.25 and 5.68 eV, respectively (Table 3).

The computed transitions of the imino form can be compared with the observed transitions of 3-methylcytidine in water solution.[47] Table 3 shows that the observed transitions near 4.64 and 5.59 eV of 3-methylcytidine can be explained in terms of the computed transitions of the imino form of cytosine within an accuracy of 0.3 eV. Therefore, the above discussion suggests that the absorption spectra of aqueous solutions of cytosine are mainly dominated by the N1H tautomer and that the contribution from other tautomers will be not significant.

3.3. Excited-State Geometries. Ground- and excited-state optimized geometrical parameters of cytosine tautomers and their hydrated forms are presented in Table 4 whereas their structures along with hydrogen bond distances are shown in Figure 2. The geometry optimizations of the lowest singlet $\pi\pi^*$ excited state of the N1H and N3H tautomers and their hydrated forms gave convergence problem with the 6-311G(d,p) and other basis sets. Earlier, we showed that the application of a mixed basis set in which the 4-31G basis set was used for all atoms except the amino nitrogen, for which the 6-311+G(d) basis set was used, is suitable in reproducing ground-state amino-group nonplanarity at the HF level and in optimizing the lowest singlet $\pi\pi^*$ and $n\pi^*$ excited states of the N1H tautomer of cytosine at the CIS level.[37] Here we have used a similar mixed basis set in the geometry optimization of the lowest singlet $\pi\pi^*$ excited state of the N1H and N3H tautomers and their hydrated forms. Furthermore, in the case of the N3H tautomer and its hydrated form, the molecular orbitals from 29 to 105 and 44 to 144, respectively, were used in CI calculations using the Read Window option of the Gaussian suite of programs.[63] Unfortunately, the geometry optimizations of the lowest singlet $\pi\pi^*$ excited state of the imino tautomer and its hydrated form and those of the hydrated N1H tautomer were not successful. As the geometry optimizations proceeded, the excitation energy went down to about 0.02 eV, and the calculation aborted because of the lack of convergence.

For the N1H tautomer in the gas phase, the amino group is pyramidal both in the ground and lowest singlet $\pi\pi^*$ excited states ($S_1(\pi\pi^*)$). Since a different basis set was used for the $\pi\pi^*$ excited-state geometry optimization, we cannot discuss the quantitative change in geometry but rather will restrict our discussion to the qualitative changes. Whereas the ground-state ring geometry is planar in the $S_1(\pi\pi^*)$ excited state, the ring is nonplanar, and such a distortion is localized mainly at the N1C6C5C4 part of the ring; the C6 atom lies appreciably away from the N1C2N3C4 plane. In the lowest singlet $n\pi^*$ excited state ($S_2(n\pi^*)$), the N3 atom lies appreciably out of the plane, and such a deformation is greater compared to earlier results obtained using the smaller basis set.[37] The amino group is also considerably rotated. Furthermore, both the amino group and the H1 hydrogen are also out of the plane and are in the cis position with respect to each other along the N1C4 direction ($\angle$H1N1C4N4 = 8.5°). The out-of-plane distortions of both of the amino groups and the H1 hydrogen atom are in opposite directions with respect to the displacement of the N3 atom. One possible reason for the out-of-plane deformation of the N3 atom in the $S_2(n\pi^*)$ state may be due to the fact that the state is mainly characterized by the excitation of the N3 lone pair; the contribution from the carbonyl group is negligible. This consideration is also supported by the fact that compared to the ground state no substantial increase in the C2O2 bond length is revealed under the geometrical relaxation of the state ($S_2(n\pi^*)$). Furthermore, because of the strong nonplanarity of the system, mixing between π and σ orbitals also cannot be ruled out. Some contribution from the amino-group nitrogen lone pair is also revealed in the relaxed $S_2(n\pi^*)$ excited state, which consequently may be responsible for the out-of-plane deformation and rotation of the amino group. Under hydration with three water molecules, the amino group is more planar in the ground state (Table 4, Figure 2). In the $S_2(n\pi^*)$ excited state, the mode of hydration around the N3 site is completely modified (Table 4, Figure 2). Thus, whereas in the ground state the N3 site makes a strong hydrogen bond with water molecules by acting as a hydrogen bond acceptor (Figure 2a), in the $S_2(n\pi^*)$ excited state, the N3 atom is very weakly bonded with water molecules (Figure 2b). The two water molecules form a cyclic hydrogen-bonded structure between the amino hydrogen and the carbonyl group in the $S_2(n\pi^*)$ state. The repulsive nature

TABLE 4: Ground- and Excited-State Optimized Bond Lengths (Å), Bond Angles (deg), and Dihedral Angles (deg) of the N1H, N3H, and Enol Tautomers of Cytosine and Their Complexes with Three Water Molecules Obtained from the 6-311G(d,p) Basis Set[a]

	N1H					N3H						enol			
	S_0		$S_1(\pi-\pi^*)$[b]	$S_2(n-\pi^*)$		S_0		$S_1(\pi-\pi^*)$[c]		$S_2(n-\pi^*)$		S_0		$S_1(\pi-\pi^*)$	
parameters		+3W			+3W		+3W		+3W		+3W		+3W		+3W
C2N1	1.403	1.388	1.459	1.375	1.355	1.366	1.352	1.334	1.353	1.383	1.359	1.314	1.317	1.346	1.350
N3C2	1.362	1.352	1.336	1.399	1.389	1.410	1.391	1.437	1.448	1.388	1.385	1.314	1.319	1.298	1.308
C4N3	1.294	1.309	1.348	1.336	1.342	1.346	1.344	1.355	1.391	1.390	1.373	1.320	1.327	1.359	1.360
C5C4	1.445	1.444	1.392	1.450	1.447	1.366	1.380	1.416	1.441	1.349	1.373	1.407	1.416	1.394	1.404
C6N1	1.347	1.348	1.350	1.398	1.403	1.290	1.304	1.359	1.329	1.334	1.352	1.329	1.336	1.354	1.351
C6C5	1.338	1.338	1.426	1.337	1.338	1.411	1.395	1.394	1.395	1.449	1.445	1.366	1.359	1.458	1.457
O2C2	1.191	1.206	1.218	1.182	1.202	1.189	1.208	1.225	1.239	1.181	1.198	1.322	1.315	1.311	1.303
N4C4	1.347	1.330	1.386	1.407	1.395	1.358	1.340	1.365	1.341	1.382	1.348	1.351	1.333	1.341	1.326
H1N1	0.994	1.000	0.995	0.994	1.000										
H3N3						0.996	1.000	0.993	1.000	0.997	0.999				
O2H2												0.944	0.953	0.944	0.956
H5C5	1.071	1.071	1.072	1.074	1.075	1.071	1.071	1.072	1.072	1.075	1.076	1.073	1.072	1.077	1.078
H6C6	1.074	1.074	1.068	1.073	1.072	1.079	1.078	1.065	1.067	1.072	1.070	1.077	1.077	1.072	1.071
H41N4	0.991	0.991	1.000	1.005	1.002	0.994	0.997	0.999	0.998	0.996	0.992	0.993	1.001	0.993	1.003
H42N4	0.993	1.003	0.999	0.998	1.002	0.993	0.991	1.002	1.010	0.999	0.998	0.991	0.991	0.992	0.992
N1C2N3	116.4	117.7	117.6	108.6	110.1	116.4	117.4	118.1	115.8	109.4	113.7	127.9	127.3	126.7	127.0
C2N3C4	120.5	120.8	121.4	119.8	118.8	124.8	124.6	118.2	104.5	121.8	119.9	116.4	117.3	111.8	112.8
N3C4C5	124.0	122.4	121.0	110.8	110.2	117.8	117.5	117.6	113.3	120.6	118.6	121.6	120.5	122.6	121.1
C2N1C6	123.2	122.2	119.5	121.8	121.2	118.4	117.9	120.8	120.8	120.6	120.2	115.0	115.0	117.1	116.1
C4C5C6	115.5	116.1	118.8	116.2	116.2	115.8	115.7	118.1	114.8	116.0	116.3	115.5	116.0	116.7	116.6
N1C6C5	120.4	120.9	115.7	121.2	120.8	126.9	126.8	119.1	119.3	110.0	108.7	123.6	123.9	106.8	108.5
N1C2O2	118.4	119.1	115.0	124.9	124.8	125.9	124.9	126.9	125.1	127.1	124.9	116.8	118.2	115.7	116.7
N3C2O2	125.2	123.2	127.4	126.4	125.0	117.8	117.7	115.0	119.1	123.5	121.3	115.3	114.5	117.6	116.3
N3C4N4	117.7	118.5	116.3	124.4	124.3	117.2	116.7	118.9	121.2	112.9	115.8	116.7	118.2	114.8	116.4
C5C4N4	118.3	119.1	122.4	122.2	123.6	125.0	125.8	123.3	125.3	126.4	125.6	121.7	121.3	122.5	122.5
C2N1H1	115.6	116.3	114.7	116.1	116.8										
C6N1H1	121.3	121.6	122.5	120.2	121.3										
C2N3H3						114.3	117.0	115.7	115.1	116.4	119.2				
C4N3H3						120.8	118.3	122.2	117.1	118.6	119.9				
C2O2H2												107.7	110.4	108.9	111.2
C4C5H5	122.2	121.8	120.9	121.4	121.3	122.2	122.1	119.5	122.2	121.3	120.5	122.2	121.8	121.1	120.1
C6C5H5	122.3	122.1	120.2	122.4	122.4	122.1	122.3	122.3	122.8	122.6	122.8	122.3	122.2	121.2	121.1
N1C6H6	116.7	116.3	120.2	115.3	115.3	115.5	115.2	117.5	117.9	123.4	120.4	115.9	115.8	118.5	118.6
C5C6H6	122.9	122.8	124.1	123.5	123.9	117.6	118.0	122.7	122.7	126.7	123.8	120.5	120.3	121.4	122.0
C4N4H41	120.8	120.2	114.6	113.5	113.9	118.2	119.1	115.4	118.4	114.0	118.4	116.8	121.6	117.3	120.9
C4N4H42	117.2	120.6	111.1	112.1	113.0	116.6	118.9	116.2	116.8	114.1	118.7	119.7	119.7	120.9	120.1
H41N4H42	118.7	118.8	111.9	109.5	110.8	114.7	118.4	112.7	117.8	111.6	118.1	117.8	118.7	118.9	118.7
N1C6C5C4	0.0	0.2	−21.2	1.2	2.6	0.4	0.9	−14.8	2.7	31.9	39.3	0.0	−0.1	−38.9	−40.2
N3C2N1C6	0.1	0.1	−20.5	−14.5	−12.4	0.5	−1.5	−3.9	−18.6	44.7	29.7	0.1	0.3	−27.1	−21.9
C4N3C2N1	−0.3	0.5	1.5	48.5	48.4	−0.6	2.8	−22.0	53.8	−8.3	11.2	−0.2	−0.7	−7.0	−11.3
C5C4N3C2	0.4	−0.8	6.6	−55.9	−56.7	0.5	−2.2	28.6	−61.9	−10.8	−22.9	0.3	0.7	14.8	15.9
C6C5C4N3	−0.2	0.4	3.2	27.7	28.4	−0.4	0.3	−10.6	36.4	−1.4	−3.9	−0.2	−0.3	9.0	10.0
O2C2N1C6	179.9	180.0	158.6	169.0	171.4	−179.5	178.3	177.7	161.4	−139.0	−152.8	179.9	179.7	154.8	158.2
N4C4N3C2	−178.5	179.5	−167.5	106.2	108.4	−177.7	178.8	−156.3	122.3	173.1	157.1	−178.5	−179.3	−164.5	−162.7
N3C2N1H1	179.8	180.0	179.3	178.9	177.4										
C5C4N3H3						177.2	179.0	−174.8	169.4	148.4	168.6				
H2O2C2N1												0.2	−1.5	−2.4	−0.8
H5C5C4N3	−179.7	−179.4	−173.9	−154.6	−154.3	179.8	−179.6	171.8	−140.3	177.3	169.1	−179.7	179.8	−159.9	153.7
H6C6C5C4	180.0	−179.9	158.4	179.2	179.7	180.0	−179.5	174.7	−176.5	146.8	−170.3	180.0	180.0	−179.1	176.2
H41N4C4N3	−8.2	−4.0	−14.9	32.9	18.6	−24.7	−12.8	−29.8	−7.0	−49.4	8.4	−11.8	2.5	−6.7	0.6
H42N4C4N3	−167.7	−176.2	−142.7	−91.8	−109.0	−167.6	−171.1	−165.1	−157.3	−179.2	163.6	−164.7	180.0	−167.3	173.7

[a] +3W represents the corresponding species hydrated with three water molecules. [b] For the 4-31G and 6-311+G(d) mixed basis sets, see text for details. [c] Using the read-window (RW) option and the 4-31G and 6-311+G(d) mixed basis sets; see text for details.

of the N3 atom in this state ($S_2(n\pi^*)$) is justified, as the lone-pair electron is promoted to antibonding orbitals.

In the case of the N3H tautomer in the ground state, although the ring geometry is planar, the amino group is more pyramidal than the corresponding state of the N1H tautomer (Table 4). In the lowest singlet $\pi\pi^*$ excited state ($S_1(\pi\pi^*)$), the N3H tautomer adopts the boat-type structure. The N1C2C4C5 atoms are approximately in one plane, and the N3 and C6 atoms are out of the plane (Table 4). In the lowest singlet $n\pi^*$ excited state ($S_2(n\pi^*)$), the geometry is twisted around the N1C2 bond, with the N1 atom being notably out of the plane from the approximate ring plane. The amino group remains pyramidal in both excited states. The ground-state amino-group pyramidalization of the N3H tautomer is decreased whereas the ring geometry is slightly nonplanar after hydration with three water molecules. After hydration, the $S_1(\pi\pi^*)$ excited-state geometrical distortion is around the C2N3 bond, and they (especially N3H) are appreciably out-of-plane. The hydrogen bond distance between the water hydrogen and N1 atom is also increased (Figure 2c). Such an increase may be either due to mixing with the $n\pi^*$ transition localized at the N1 lone pair or due to the limited number of orbitals considered in the configuration. In the $S_2(n\pi^*)$ excited state, the hydration structure is completely modified (Figure 2d). The water molecule in not bonded between the carbonyl group and N1 site; instead, all three water molecules are bonded at the C2O, N3H, and amino-group sites (Figure 2d). Such a change of hydration structure in the $n\pi^*$ state is in accordance with the established fact that hydrogen bonds are largely destabilized under such excitations.[39−41]

In the case of the enol tautomer in the ground state, the amino

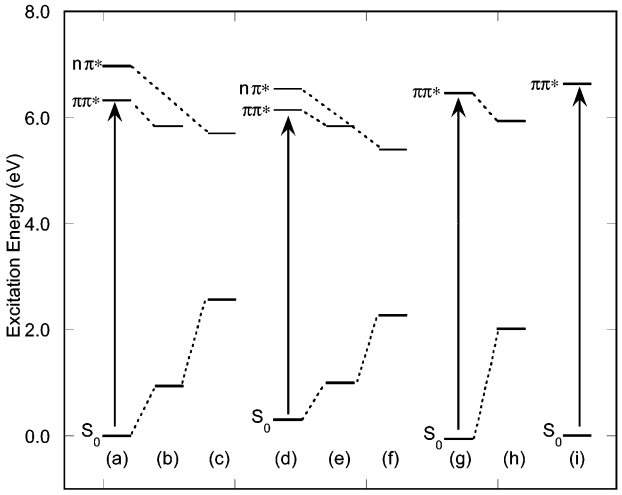

Figure 3. Energy-level diagram of isolated cytosine tautomers. (a), (d), (g), and (i) represent vertical states of the N1H, N3H, enol, and imino tautomers, respectively; (b), (e), and (h) represent optimized lowest singlet $\pi\pi^*$ excited state of the N1H, N3H, and enol tautomers, respectively; whereas (c) and (f) represent the optimized lowest singlet nπ^* excited state of the N1H and N3H tautomers, respectively.

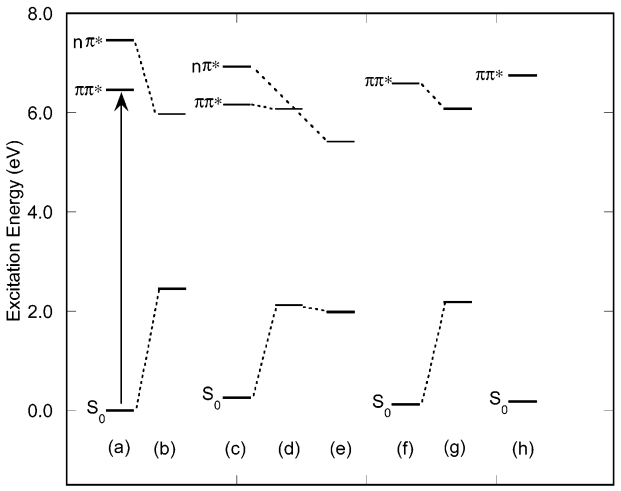

Figure 4. Energy-level diagram of hydrated cytosine tautomers. (a), (c), (f), and (h) represent the vertical states of the hydrated N1H, N3H, enol, and imino forms, respectively; (b) and (e) represent the optimized lowest singlet nπ^* excited state of the hydrated N1H and N3H tautomers, respectively; and (d) and (g) represent the optimized lowest singlet $\pi\pi^*$ excited state of the hydrated N3H and enol tautomer, respectively.

group pyramidalization is larger than for the N1H tautomer but lower than for the N3H tautomer. In the lowest singlet $\pi\pi^*$ excited state (S1($\pi\pi^*$)), the ring geometry is largely distorted, especially around the C5C6 bond. The C6H group is displaced appreciably out of the plane. The C5C6 bond length is also increased notably by about 0.092 Å compared to the ground-state value (Table 4). Furthermore, the amino-group pyramidalization is also reduced in the excited state. Hydration of the enol tautomer significantly reduces the amino-group pyramidalization in the ground state (Table 4). The geometrical deformation of the hydrated enol form in the $S_1(\pi\pi^*)$ excited state is revealed to be similar to the isolated tautomer (Table 4).

3.4. Phototautomerism. The energy-level diagrams containing the lowest singlet $\pi\pi^*$ and nπ^* states of cytosine tautomers and their hydrated forms obtained at the CIS level are shown in Figures 3 and 4, respectively. The excitation energies displayed in the energy-level diagrams were computed using the 6-311G(d,p) basis set utilizing geometries optimized at different levels and basis sets as discussed earlier. The energy-level diagrams suggest that among the vertical singlet $\pi\pi^*$ excited states the state corresponding to the N3H tautomer is the lowest both in the gas phase and after hydration (Figures 3 and 4). The ordering of the $\pi\pi^*$ and nπ^* states of the N1H and N3H tautomers is also changed as a result of the excited-state geometry relaxation. Consequently, the nπ^* excited state of the N1H and N3H tautomers lies lowest under the geometry relaxation (Figures 3 and 4). However, one can argue that such a change of the relative position of these two states ($\pi\pi^*$ and nπ^*) may be due to the different basis sets used in the geometry optimization and CIS calculation of excitation energies. However, the effect of using different basis sets may not be important in this case since similar results were found in an earlier study in which the ground- and excited-state calculations were performed with the same basis set.[37] Such a crossing of the $\pi\pi^*$ and nπ^* states may be responsible for the nonradiative decay and thus the weak fluorescence of the compound.[10,11] The energy-level diagram clearly indicates that, in the gas phase and under hydration, energy transfer will take place from the lowest $\pi\pi^*$ state of the enol form (in the gas phase) or the N1H tautomer (in an aqueous solution) to the corresponding state of the N3H tautomer. Thus, it follows from our calculations that under electronic excitation, cytosine would phototautomerize to the N3H form. The computed energy differences between the optimized $S_1(\pi\pi^*)$ state and the ground state lying vertically below it for the N1H and N3H tautomers are 4.90 and 4.84 eV, respectively, and the corresponding scaled (scaling factor 0.72) values would be 3.53 and 3.48 eV, respectively. These values are closer to the experimental fluorescence peak observed near 3.85 eV (322 nm).[10] It appears that both the N1H and N3H tautomers are responsible for the fluorescence of the cytosine.

4. Conclusions

In the ground state, the enol tautomeric form of the cytosine is the most stable in the gas phase. However, under hydration, the N1H amino−oxo form is the most stable. The amino group is found to be the most pyramidal in the N3H tautomeric form. Under hydration, amino-group nonplanarity is reduced. Although the ring geometries of tautomers are planar in the ground state, excited-state geometries are found to be substantially nonplanar both in the $\pi\pi^*$ and nπ^* singlet excited states. It is found that the absorption of cytosine is dominated mainly by the N1H tautomer. The singlet nπ^* excitation has an appreciable effect on the hydrated geometries of cytosine tautomers, leading to a substantial modification of the mode of interaction of water molecules with cytosine tautomers. Cytosine is suggested to be phototautomerized to the N3H form both in the gas phase and under hydration. However, both the N1H and N3H tautomers would involve the fluorescence of cytosine.

Acknowledgment. We are thankful to NIH-RCMI for grant no. G1 2RR13459-21, NSF-CREST for grant nos.9805465 and 9706268, and ONR for grant no. N00014-98-1-0592 for financial assistance. We are also thankful to the Mississippi Center for Supercomputing Research for the use of the computational facilities.

References and Notes

(1) Leszczynski, J. In *Advances in Molecular Structure and Research*; Hargittai, M., Hargittai, I., Eds.; JAI Press: Stamford, CT, 2000; Vol 6, p 209.

(2) Leszczynski, J. In *The Encyclopedia of Computational Chemistry*; John Wiley & Sons: New York, 1998; Vol. 5, p 2951.

(3) Gorb, L.; Leszczynski, J. In *Computational Molecular Biology;* Leszczynski, J., Ed.; Theoretical and Computational Chemistry; Elsevier: Amsterdam, 1999; Vol 8, p 167.

(4) Hobza, P.; Sponer, J.; Leszczynski, J. In *Computational Molecular Biology;* Leszczynski, J., Ed.; Theoretical and Computational Chemistry; Elsevier: Amsterdam, 1999; Vol 8, p 85.

(5) Nowak, M. J.; Lapinski, L.; Kwiatkowski, J. S.; Leszczynski, J. In *Computational Chemistry: Reviews of Current Trends*; Leszczynski, J., Ed.; World Scientific: Singapore, 1997; Vol 2, p 140.

(6) Sponer, J.; Hobza, P.; Leszczynski, J. In *Computational Chemistry: Reviews of Current Trends*; Leszczynski, J., Ed.; World Scientific: Singapore, 2000; Vol 5, p 171.

(7) Sambrano, J. R.; de Souza, A. R.; Queralt, J. J.; Andres, J. *Chem. Phys. Lett.* **2000**, *317*, 437.

(8) Nishio, H.; Ono, A.; Matsuda, A.; Ueda, T. *Nucleic Acids Res.* **1992**, *20*, 777.

(9) Singer, B.; Chavez, F.; Goodman, M. F.; Essigmann, J. M.; Dosanjh, M. K. *Proc. Natl. Acad. Sci. U.S.A.* **1989**, *86*, 8271.

(10) Callis, P. R. *Annu. Rev. Phys. Chem.* **1983**, *34*, 329.

(11) Eisinger, J.; Lamola, A. A. In *Excited States of Proteins and Nucleic Acids*; Steiner, R. F., Weinryb, I., Eds.; Plenum Press: New York, 1971; p 107.

(12) Pecourt, J.-M. L.; Peon, J.; Kohler, B. *J. Am. Chem. Soc.* **2001**, *123*, 10370.

(13) Mishra, P. C. *J. Mol. Struct.* **1989**, *195*, 201.

(14) Mishra, S. K.; Shukla, M. K.; Mishra, P. C. *Spectrochim. Acta, Part A* **2000**, *56*, 1355.

(15) Broo, A. *J. Phys. Chem. A* **1998**, *102*, 526.

(16) Szczesniak, M.; Szczepaniak, K.; Kwiatowski, J. S.; KuBulat, K.; Person, W. B. *J. Am. Chem. Soc.* **1988**, *110*, 8319.

(17) Kwiatkowski, J. S.; Leszczynski, J. *J. Phys. Chem.* **1996**, *100*, 941.

(18) Smets, J.; Adamowicz, L.; Maes, G. *J. Phys. Chem.* **1996**, *100*, 6434.

(19) Brown, R. D.; Godfrey, P. D.; McNaughton, D.; Pierlot, A. P. *J. Am. Chem. Soc.* **1989**, *111*, 2308.

(20) Drefus, M.; Bensaude, O.; Dodin, G.; Dubois, J. E. *J. Am. Chem. Soc.* **1976**, *98*, 6338.

(21) McClure, R. J.; Craven, B. M. *Acta Crystallogr., Sect. B* **1973**, *29*, 1234.

(22) Kobayashi, R. *J. Phys. Chem. A* **1998**, *102*, 10813.

(23) Gorb, L.; Podolyan, Y.; Leszczynski, J. *J. Mol. Struct.: THEOCHEM* **1999**, *487*, 47.

(24) Estrin, D. A.; Paglieri, L.; Corongiu, G. *J. Phys. Chem.* **1994**, *98*, 5653.

(25) Chandra, A. K.; Nguyen, M. T.; Zeegers-Huyskens, Th. *J. Mol. Struct.: THEOCHEM* **2000**, *519*, 1.

(26) Wolf, B.; Hanlon, S. *Biochemistry* **1975**, *14*, 1661.

(27) Hearst, J. *Biopolymers* **1965**, *3*, 57.

(28) Falk, M.; Hartman, K. A.; Lord, R. C. *J. Am. Chem. Soc.* **1962**, *84*, 3843.

(29) Falk, M.; Poole, A. G.; Goymour, C. G. *Can. J. Chem.* **1970**, *48*, 1536.

(30) Brandes, R.; Rupprecht, A.; Kearns, D. R. *J. Biophys. (Tokyo)* **1989**, *56*, 683.

(31) Gorb, L.; Leszczynski, J. *Int. J. Quantum Chem.* **1998**, *70*, 855.

(32) Shishkin, O. V.; Gorb, L.; Leszczynski, J. *J. Phys. Chem. B* **2000**, *104*, 5357.

(33) van Mourik, T.; Benoit, D. M.; Price, S. L.; Clary, D. C. *Phys. Chem. Chem. Phys.* **2000**, *2*, 1281.

(34) Aleman, C. *Chem. Phys. Lett.* **1999**, *302*, 461.

(35) Brady, B. B.; Peteanu, L. A.; Levy, D. H. *Chem. Phys. Lett.* **1988**, *147*, 538.

(36) Chinsky, L.; Laigle, A.; Peticolas, L.; Turpin, P.-Y. *J. Chem. Phys.* **1982**, *76*, 1.

(37) Shukla, M. K.; Mishra, P. C. *Chem. Phys.* **1999**, *240*, 319.

(38) Danilov, V. I.; Slyusarchuk, O. N.; Alderfer, J. L.; Stewart, J. J. P.; Callis, P. R. *Photochem. Photobiol.* **1994**, *59*, 125.

(39) Shukla, M. K.; Mishra, P. C. *Chem. Phys.* **1998**, *230*, 187.

(40) Shukla, M. K.; Leszczynski, J. *J. Phys. Chem. A* **2002**, *106*, 1011.

(41) Kim, N. J.; Kang, H.; Jeong, G.; Kim, Y. S.; Lee, K. T.; Kim, S. K. *J. Phys. Chem. A* **2000**, *104*, 6552.

(42) Korter, T. M.; Pratt, D. W.; Kupper, J. *J. Phys. Chem. A* **1998**, *102*, 7211.

(43) Foresman, J. B.; Head-Gordon, M.; Pople, J. A.; Frisch, M. J. *J. Phys. Chem.* **1992**, *96*, 135.

(44) (a) Casida, M. E.; Jamorski, C.; Casida, K. C.; Salahub, D. R. *J. Chem. Phys.* **1998**, *108*, 4439. (b) Robb, M. A.; Garavelli, M.; Olivucci, M.; Bernardi, F. In *Reviews in Computational Chemistry*; Lipkowitz, K. B., Boyd, D. B., Eds.; Wiley-VCH: New York, 2000; Vol 15, p 87.

(45) (a) Frisch, M. J.; Trucks, G. W.; Schlegel, H. B.; Gill, P. M. W.; Johnson, B. G.; Robb, M. A.; Cheeseman, J. R.; Keith, T.; Petersson, G. A.; Montgomery, J. A.; Raghavachari, K.; Al-Laham, M. A.; Zakrzewski, V. G.; Ortiz, J. V.; Foresman, J. B.; Cioslowski, J.; Stefanov, B. B.; Nanayakkara, A.; Challacombe, M.; Peng, C. Y.; Ayala, P. Y.; Chen, W.; Wong, M. W.; Andres, J. L.; Replogle, E. S.; Gomperts, R.; Martin, R. L.; Fox, D. J.; Binkley, J. S.; Defrees, D. J.; Baker, J.; Stewart, J. P.; Head-Gordon, M.; Gonzalez, C.; Pople, J. A. *Gaussian 94*, revision E.2; Gaussian, Inc.: Pittsburgh, PA, 1995. (b) Frisch, M. J.; Trucks, G. W.; Schlegel, H. B.; Scuseria, G. E.; Robb, M. A.; Cheeseman, J. R.; Zakrzewski, V. G.; Montgomery, J. A., Jr.; Stratmann, R. E.; Burant, J. C.; Dapprich, S.; Millam, J. M.; Daniels, A. D.; Kudin, K. N.; Strain, M. C.; Farkas, O.; Tomasi, J.; Barone, V.; Cossi, M.; Cammi, R.; Mennucci, B.; Pomelli, C.; Adamo, C.; Clifford, S.; Ochterski, J.; Petersson, G. A.; Ayala, P. Y.; Cui, Q.; Morokuma, K.; Malick, D. K.; Rabuck, A. D.; Raghavachari, K.; Foresman, J. B.; Cioslowski, J.; Ortiz, J. V.; Stefanov, B. B.; Liu, G.; Liashenko, A.; Piskorz, P.; Komaromi, I.; Gomperts, R.; Martin, R. L.; Fox, D. J.; Keith, T.; Al-Laham, M. A.; Peng, C. Y.; Nanayakkara, A.; Gonzalez, C.; Challacombe, M.; Gill, P. M. W.; Johnson, B. G.; Chen, W.; Wong, M. W.; Andres, J. L.; Head-Gordon, M.; Replogle, E. S.; Pople, J. A. *Gaussian 98*, revision A.6; Gaussian, Inc.: Pittsburgh, PA, 1998. (c) Frisch, M. J.; Trucks, G. W.; Schlegel, H. B.; Scuseria, G. E.; Robb, M. A.; Cheeseman, J. R.; Zakrzewski, V. G.; Montgomery, J. A., Jr.; Stratmann, R. E.; Burant, J. C.; Dapprich, S.; Millam, J. M.; Daniels, A. D.; Kudin, K. N.; Strain, M. C.; Farkas, O.; Tomasi, J.; Barone, V.; Cossi, M.; Cammi, R.; Mennucci, B.; Pomelli, C.; Adamo, C.; Clifford, S.; Ochterski, J.; Petersson, G. A.; Ayala, P. Y.; Cui, Q.; Morokuma, K.; Malick, D. K.; Rabuck, A. D.; Raghavachari, K.; Foresman, J. B.; Cioslowski, J.; Ortiz, J. V.; Stefanov, B. B.; Liu, G.; Liashenko, A.; Piskorz, P.; Komaromi, I.; Gomperts, R.; Martin, R. L.; Fox, D. J.; Keith, T.; Al-Laham, M. A.; Peng, C. Y.; Nanayakkara, A.; Gonzalez, C.; Challacombe, M.; Gill, P. M. W.; Johnson, B. G.; Chen, W.; Wong, M. W.; Andres, J. L.; Head-Gordon, M.; Replogle, E. S.; Pople, J. A. *Gaussian 98*, revision A.9; Gaussian, Inc.: Pittsburgh, PA, 1998.

(46) Chahinian, M.; Seba, H. B.; Ancian, B. *Chem. Phys. Lett.* **1998**, *285*, 337.

(47) Kaito, A.; Hatano, M.; Ueda, T.; Shibuya, S. *Bull. Chem. Soc. Jpn.* **1980**, *53*, 3073.

(48) Zaloudek, F.; Novros, J. S.; Clark, L. B. *J. Am. Chem. Soc.* **1985**, *107*, 7344.

(49) Johnson, W. C., Jr.; Vipond, P. M.; Girod, J. C. *Biopolymers* **1971**, *10*, 923.

(50) Raksany, K.; Foldvary, I. *Biopolymers* **1978**, *17*, 887.

(51) Fulscher, M. P.; Roos, B. O. *J. Am. Chem. Soc.* **1995**, *117*, 2089.

(52) Petke, J. D.; Maggiora, G. M.; Christoffersen, R. E. *J. Phys. Chem.* **1992**, *96*, 6992.

(53) Clark, L. B.; Tinico, I. *J. Am. Chem. Soc.* **1965**, *87*, 11.

(54) Miles, D. W.; Robins, R. K.; Eyring, H. *Proc. Natl. Acad. Sci. U.S.A.* **1967**, *57*, 1138.

(55) Voelter, W.; Records, R.; Bunnenberg, E.; Djerassi, C. *J. Am. Chem. Soc.* **1968**, *90*, 6113.

(56) Callis, P. R.; Simpson, W. T. *J. Am. Chem. Soc.* **1970**, *92*, 3593.

(57) Lewis, T. P.; Eaton, W. A. *J. Am. Chem. Soc.* **1971**, *93*, 2054.

(58) Matsuoks, Y.; Norden, B. *J. Phys. Chem.* **1982**, *86*, 1378.

(59) Bott, C. C.; Kurucsev, T. *Spectrosc. Lett.* **1977**, *10*, 495.

(60) Callis, P. R.; Simpson, W. T. *J. Am. Chem. Soc.* **1970**, *92*, 3593.

(61) Wilson, R. W.; Callis, P. R. *J. Phys. Chem.* **1976**, *80*, 2280.

(62) Fucaloro, A. F.; Forster, L. S. *J. Am. Chem. Soc.* **1971**, *93*, 6443.

(63) Frisch, M. J.; Frisch, S.; Foresman, J. B. *Gaussian 94 User's Reference;* Gaussian, Inc.: Pittsburgh, PA, 1994; p 102.